Molecular Neurobiology (2019) 56:367–377
https://doi.org/10.1007/s12035-018-1088-7

Identification of Alprenolol Hydrochloride as an Anti-prion Compound Using Surface Plasmon Resonance Imaging

Yukiko Miyazaki[1,2] · Takeshi Ishikawa[2,3] · Yuji O. Kamatari[4] · Takehiro Nakagaki[1] · Hanae Takatsuki[5] · Daisuke Ishibashi[1] · Kazuo Kuwata[6] · Noriyuki Nishida[1] · Ryuichiro Atarashi[5]

Received: 26 July 2017 / Accepted: 15 April 2018 / Published online: 27 April 2018

Abstract

Prion diseases are transmissible neurodegenerative disorders of humans and animals, which are characterized by the aggregation of abnormal prion protein (PrP^{Sc}) in the central nervous system. Although several small compounds that bind to normal PrP (PrP^{C}) have been shown to inhibit structural conversion of the protein, an effective therapy for human prion disease remains to be established. In this study, we screened 1200 existing drugs approved by the US Food and Drug Administration (FDA) for anti-prion activity using surface plasmon resonance imaging (SPRi). Of these drugs, 31 showed strong binding activity to recombinant human PrP, and three of these reduced the accumulation of PrP^{Sc} in prion-infected cells. One of the active compounds, alprenolol hydrochloride, which is used clinically as a β-adrenergic blocker for hypertension, also reduced the accumulation of PrP^{Sc} in the brains of prion-infected mice at the middle stage of the disease when the drug was administered orally with their daily water from the day after infection. Docking simulation analysis suggested that alprenolol hydrochloride fitted into the hotspot within mouse PrP^{C}, which is known as the most fragile structure within the protein. These findings provide evidence that SPRi is useful in identifying effective drug candidates for neurodegenerative diseases caused by abnormal protein aggregation, such as prion diseases.

Keywords Prion diseases · Surface plasmon resonance imaging · Alprenolol hydrochloride · Docking simulation

Noriyuki Nishida and Ryuichiro Atarashi contributed equally to this work.

Electronic supplementary material The online version of this article (https://doi.org/10.1007/s12035-018-1088-7) contains supplementary material, which is available to authorized users.

✉ Noriyuki Nishida
noriyukinishida@icloud.com

✉ Ryuichiro Atarashi
ryuichiro_atarashi@med.miyazaki-u.ac.jp

1 Department of Molecular Microbiology and Immunology, Graduate School of Biomedical Sciences, Nagasaki University, Nagasaki, Japan

2 Program for Nurturing Global Leaders in Tropical and Emerging Infectious Diseases, Graduate School of Biomedical Sciences, Nagasaki University, Nagasaki, Japan

3 Molecular Epidemiology, Graduate School of Biomedical Sciences, Nagasaki University, Nagasaki, Japan

4 Life Science Research Center, Gifu University, Gifu, Japan

5 Division of Microbiology, Department of Infectious Diseases, Faculty of Medicine, University of Miyazaki, Miyazaki, Japan

6 United Graduate School of Drug Discovery and Medical Information Sciences, Gifu University, Gifu, Japan

Introduction

Prion diseases are transmissible neurodegenerative disorders, which include Creutzfeldt–Jakob disease (CJD) and Gerstmann–Sträussler–Scheinker disease in humans, scrapie in sheep, and bovine spongiform encephalopathy (BSE) in cattle. The infectious agent responsible for these diseases is misfolded and aggregated prion protein (PrP^{Sc}), which is generated by conformational changes in cellular prion protein (PrP^{C}) [1, 2].

Effective therapeutics have not been established for human prion diseases, despite decades of research. The drugs that have been identified target several different stages of the prion infection process: conformation changes in PrP, clearance of aggregated PrPs, and signaling pathways leading to neurodegeneration [3–5]. Quinacrine inhibited the conversion process by binding to PrP^{C}, leading to reduced PrP^{Sc} accumulation in prion-infected cultured cells [6, 7]; however, it exhibited non-significant therapeutic effects on CJD patients and showed side effects such as liver dysfunction and skin rashes [8, 9]. Pentosan polysulfate was also reported to suppress PrP conversion by interfering with the interaction between PrP^{C} and

PrP^{Sc} [10, 11]. Intraventricular infusion of pentosan polysulfate significantly prolonged survival in animals [12, 13], but it also showed adverse effects such as seizures due to the slow metabolism of the drug [13], and therefore, this drug was not approved for human use, even by intraventricular administration [12, 14]. Doxycycline was effective in prion-infected cultured cells and in animals, but its administration did not affect the survival time of CJD patients [15–17]. Anti-PrP antibodies prevented prion pathogenesis in mice, but problems such as neurotoxicity and impermeability to the blood–brain barrier were encountered [18–21]. Several compounds targeting intracellular protein degradation systems, such as autophagy or signaling pathways related to the unfolded protein response, were reported to show anti-prion effects [22–24]. However, some of these led to toxicity in humans because they also acted on the original molecular functions in normal tissues and cells, leading to the disruption of cellular homeostasis [24, 25].

Recently, in silico studies have been conducted to identify novel PrP-binding compounds. Hotspot residues responsible for conformational changes in PrP^{C} were identified, and a lead compound designated GN8 was characterized as an anti-prion compound that interacts with this site [26]. Based on these findings, further studies involving a structure-based drug discovery approach using docking simulations identified drug candidates that targeted the hotspot and exerted anti-prion effects on prion-infected cells and mice [27, 28]. In this study, we conducted screening of 1200 FDA-approved drugs by surface plasmon resonance imaging (SPRi) to identify molecules able to bind to recombinant PrP. SPRi has recently been developed to overcome the limitation of conventional SPR in terms of high-throughput screening. Conventional SPR involves only a small number of flow cells on its sensor chip, whereas SPRi can visualize the whole surface image of a sensor chip to detect reflection changes arising from molecular binding events between immobilized small molecules and flowing proteins via the use of a charge-coupled device (CCD) camera. SPRi therefore allows for multiplex detection and high-throughput screening of molecular interactions by a single run using an array format sensor chip [29, 30]. This reverse SPR technology has been used to identify binding molecules to specifically target proteins [29, 31]. After SPRi screening, we evaluated the anti-prion activity of the hit compounds by quantifying PrP^{Sc} in prion-infected cultured cells and mice.

Methods

Compounds

Esmolol hydrochloride, dequalinium dichloride, fosinopril, antimycin A, and oxprenolol hydrochloride were purchased from Santa Cruz Biotechnology. Alexidine dihydrochloride, merbromin, candesartan, amphotericin B, alprenolol hydrochloride, triprolidine hydrochloride, methacycline hydrochloride, cefixime, and ethacrynic acid were purchased from Sigma-Aldrich. Demecarium bromide and cefoperazone were purchased from AK Scientific. Bisoprolol fumarate was purchased from MedChem Express. Benzbromarone, etifenin, cefotetan, and rebamipide were purchased from Tokyo Chemical Industry Co., Ltd. Atractyloside potassium salt was purchased from Toronto Research Chemicals. Furosemide and indomethacin were purchased from Nacalai Tesque. Acemetacin, ketoprofen, bumetanide, colistin sulfate, tranilast, norfloxacin, and doxepin hydrochloride were purchased from LKT Laboratories, Inc.

Cell Culture

Mouse neuroblastoma Neuro 2a (N2a) cells were obtained from the American Type Culture Collection (CCL 131). N2a-FK cells are PrP^{C}-overexpressing N2a cells (N2a58 cells) that are persistently infected with mouse-adapted Gerstmann–Sträussler–Scheinker strain, Fukuoka-1, as previously described. They were cultured at 37 °C under 5% CO_2 with Dulbecco's modified Eagle's medium (Wako), including 10% heat-inactivated fetal bovine serum, 100 units/mL penicillin, and 100 μg/mL streptomycin (Nacalai Tesque).

Cell-Based Screening of the Compounds

N2a-FK cells were seeded on 12 well plates at 1.5×10^5 cells/well. The next day, the cells were washed with PBS and the medium was replaced with fresh medium containing each of the sample compounds. Medium containing DMSO for the DMSO-dissolved compounds or water for the water-dissolved compounds was added to the control wells. After 48 h of incubation, the cells were washed with PBS and lysed with lysis buffer (50 mM Tris-HCl pH 7.5, 150 mM NaCl, 0.5% Triton X-100, 0.5% sodium deoxycholate, 2 mM EDTA). Then the lysate was centrifuged for 1 min at 5000 rpm and the supernatant was collected for immunoblotting.

In addition, N2a-FK cells were cultured in medium mixed with 50 μM of alprenolol hydrochloride, 100 μM of bisoprolol fumarate, or 100 μM of colistin sulfate and passaged every 3 days. As a negative control, N2a-FK cells were cultured in original medium. The cell lysates were collected every passage and total protein was prepared as described above.

Animal Infection Experiments

Three-week-old CD-1 mice were purchased from SLC (Hamamatsu, Japan). They were intracerebrally inoculated with 20 μL of 10% (*w*/*v*) brain homogenate from the affected

mice with Fukuoka-1 at 4 weeks of age. The day after infection, the powdery components of Skajilol capsules (Kotobuki Pharmaceutical Co., Ltd), which contain alprenolol hydrochloride as a major active constituent, were added to the drinking water at 250 or 50 mg/L. Mice in the control group were given drinking water without the drug. At 115 d.p.i or the terminal stage, some of mice in each group were dissected to separate out their brain tissues (at 115 d.p.i., control: $n = 3$; 250 mg/L: $n = 5$; 50 mg/L: $n = 3$, at the terminal stage, control: $n = 4$; 250 mg/L: $n = 4$; 50 mg/L: $n = 4$). All of these experiments were approved by the Committee on the Animal Care and Use Committees of Nagasaki University. The mice were cared for according to the Guidelines for Animal Experimentation of Nagasaki University.

Preparation of Brain Homogenates

Mouse brain tissues were homogenized in PBS at 20% (*w*/*v*) by Multi-Beads Shocker (Yasui Kikai). Then, 10% brain homogenates for immunoblotting were prepared by mixing with an equal volume of 2× lysis buffer.

Immunoblotting

The total protein concentration contained in the cell lysates and the brain homogenates was measured using the BCA Protein Assay Kit (Pierce). To digest PrP^C, the samples were reacted with 20 μg/mL proteinase K (PK) for 30 min at 37 °C. After denaturation by SDS sample buffer (50 mM Tris-HCl pH 6.8, 5% glycerol, 1.6% SDS, 100 mM dithiothreitol) for 10 min at 95°C, 100 μg (cell lysates) or 50 μg (brain homogenates) of each sample was applied to 15% acrylamide gel for SDS-PAGE. The protein bands were then transferred to PVDF membrane. For blocking, the membrane was placed in 5% (*w*/*v*) skim milk with TBST (10 mM Tris-HCl pH 7.8, 100 mM NaCl, 0.1% Tween 20) for 1 h. For PrP detection, the membrane was then incubated with primary antibodies: M-20 (Santa Cruz Biotechnology) or SAF83 (SPI-Bio) diluted with 1% skim milk. Then, the membrane was further reacted with secondary antibodies: horseradish peroxidase-conjugated anti-goat (Santa Cruz Biotechnology) or anti-mouse IgG antibodies (GE Healthcare Life Sciences) diluted with 1% skim milk, and the bands were visualized using the ECL Prime Western Blotting Detection Kit (GE Healthcare Life Sciences) or Clarity Wester ECL Substrate (BioRad). The intensity of each band was quantified using the ImageJ software (National Institutes of Health).

Histopathological Analysis

The hemispheres of fixed mouse brain tissues in 10% neutral buffered formalin were embedded in paraffin after dehydration treatment. The paraffin blocks were sliced into 3-μm slices and the slices were placed on microscope slides. After deparaffinization, hematoxylin–eosin staining was performed to evaluate the level of spongiform change. To quantify the area occupied by vacuolation, the white areas in an image (670 μm × 890 μm) from each brain region (cortex, thalamus, hippocampus, and striatum) were measured using the ImageJ software and compared with the whole area of the image. The hydrolytic autoclaving and formic acid method for PrP^{Sc} immunohistochemical staining has been described previously [32].

Preparation of Recombinant PrP

Expression and purification of recombinant human PrP 90–231 ($rHuPrP_{90–231}$), recombinant human PrP 23–231 ($rHuPrP_{23–231}$), and mouse PrP 23–231 ($rMoPrP_{23–231}$) in *Escherichia coli* strain BL21 (DE3) (Stratagene) was performed as previously described [33]. The purified protein was stored at − 80°C.

SPRi Screening

SPR screening to discover drugs that bind to $rHuPrP_{90–231}$ was performed by Plexera LCC (WA, USA). The screening subject was a library containing 1200 small molecules, all of which were already approved drugs by the FDA and were selected for their high chemical and pharmacological diversity, as well as for their known bioavailability and safety in humans. The sample compounds, positive (10 mM rapamycin) and negative (DMSO) controls, were printed on to the activated 3D sensor chip and immobilized by a photo-crossing reaction. Excess unbound samples were eliminated by rinsing with dimethylformamide, ethanol, and H_2O, respectively. Sample analysis was prioritized using $rHuPrP_{90–231}$ (100, 200, 400, 800 nM), then FKBP12 (100 nM) as the positive control. The protein was injected once at a flow rate of 2 μL/s. The association duration was 300 s and dissociation duration was 300 s. Subsequent regeneration was performed using 900 μL of 10 mM glycine-HCl (pH 2.0). The assay was performed using Plexera PlexArray SPRi instrumentation, visualized using the Instrument Control software, and analyzed using the Plexera Data Explorer software.

Conventional SPR Analysis

Conventional SPR analysis was performed using the Biacore T200 system (GE Healthcare Life Sciences). $rHuPrP_{23–231}$ and $rMoPrP_{23–231}$ were immobilized on a CM5 sensor chip (GE Healthcare Life Sciences) by amine coupling. Blank flow paths remained for background data. Twofold serial dilutions of alprenolol hydrochloride,

Table 1 Hit compounds by SPRi screening

	Drugs	Avg K_D (M)	Avg k_a (1/Ms)	Avg k_d (1/s)	Therapeutic class	Therapeutic effect
1	Esmolol hydrochloride	1.77×10^{-10}	1.58×10^{5}	2.81×10^{-5}	Cardiovascular	Antiarrhythmic
2	Alexidine dihydrochloride	2.26×10^{-10}	1.76×10^{3}	3.97×10^{-7}	Infectiology	Antibacterial
3	Dequalinium dichloride	4.81×10^{-10}	285	1.37×10^{-7}	Infectiology	Antibacterial
4	Demecarium bromide	1.69×10^{-9}	2.14×10^{3}	3.60×10^{-6}	Ophthalmology	Antiglaucoma
5	Bisoprolol fumarate	2.78×10^{-9}	307	8.54×10^{-7}	Cardiovascular	Antianginal
6	Benzbromarone	3.45×10^{-9}	1.10×10^{5}	3.78×10^{-4}	Cardiovascular	Antianginal
7	Atractyloside potassium salt	3.58×10^{-9}	2.68×10^{5}	9.59×10^{-4}	Oncology	Antineoplastic
8	Fosinopril	5.46×10^{-9}	7.04×10^{4}	3.84×10^{-4}	Cardiovascular	Antihypertensive
9	Merbromin	6.50×10^{-9}	72.7	4.72×10^{-7}	Infectiology	Antibacterial
10	Furosemide	7.25×10^{-9}	9.12×10^{4}	6.61×10^{-4}	Metabolism	Antihypertensive
11	Etifenin	1.00×10^{-8}	1.00×10^{3}	1.00×10^{-5}	Diagnostic	Chemosensitizer
12	Acemetacin	1.04×10^{-8}	5.19×10^{4}	5.42×10^{-4}	Metabolism	Anti-inflammatory
13	Candesartan	1.05×10^{-8}	2.06×10^{3}	2.17×10^{-5}	Cardiovascular	Antihypertensive
14	Amphotericin B	1.11×10^{-8}	1.59×10^{5}	1.75×10^{-3}	Infectiology	Antibacterial
15	Alprenolol hydrochloride	1.14×10^{-8}	4.86×10^{4}	5.53×10^{-4}	Cardiovascular	Antianginal
16	Ketoprofen	1.23×10^{-8}	1.68×10^{5}	2.07×10^{-3}	Central nervous system	Analgesic
17	Bumetanide	1.43×10^{-8}	1.61×10^{5}	2.31×10^{-3}	Metabolism	Diuretic
18	Triprolidine hydrochloride	1.67×10^{-8}	6.08×10^{4}	1.02×10^{-3}	Allergology	Antihistaminic
19	Methacycline hydrochloride	1.92×10^{-8}	244	4.67×10^{-6}	Metabolism	Antibacterial
20	Cefoperazone dihydrate	2.36×10^{-8}	1.39×10^{5}	3.28×10^{-3}	Infectiology	Antibacterial
21	Colistin sulfate	2.37×10^{-8}	6.42×10^{4}	1.52×10^{-3}	Infectiology	Antibacterial
22	Cefixime	2.39×10^{-8}	7.60×10^{4}	1.82×10^{-3}	Infectiology	Antibacterial
23	Tranilast	2.43×10^{-8}	4.44×10^{4}	1.08×10^{-3}	Allergology	Antiallergic
24	Norfloxacin	2.45×10^{-8}	3.90×10^{4}	9.54×10^{-4}	Infectiology	Antibacterial
25	Antimycin A	5.57×10^{-8}	6.18×10^{4}	3.45×10^{-3}	Infectiology	Antibacterial
26	Cefotetan	7.85×10^{-8}	2.44×10^{4}	1.91×10^{-3}	Infectiology	Antibacterial
27	Indomethacin	1.04×10^{-7}	6.81×10^{4}	7.09×10^{-3}	Central nervous system	Analgesic
28	Doxepin hydrochloride	1.49×10^{-7}	3.30×10^{4}	4.91×10^{-3}	Allergology	Anticonvulsant
29	Oxprenolol hydrochloride	3.08×10^{-7}	32.7	1.01×10^{-5}	Cardiovascular	Antianginal
30	Ethacrynic acid	9.54×10^{-7}	582	5.55×10^{-4}	Metabolism	Diuretic
31	Rebamipide	1.86×10^{-6}	338	6.29×10^{-4}	Metabolism	Antiulcer

In total, 31 compounds with an K_D value less than 1×10^{-6} M were listed as hit compounds

bisoprolol fumarate, and ampicillin (each at 625, 313, 156, 78, 39, 20, and 0 μM), and quinacrine (500, 250, 125, 62.5, 31.2, 15.6, 7.8, 3.9, and 0 μM) in running buffer (0.01 M HEPES pH 7.4, 0.15 M NaCl, 0.005% (*v*/*v*) Tween20) were injected for 120 s at a flow rate of 30 μL/min. After injection of each sample, the same buffer alone was injected for 60 s at a flow rate of 30 μL/min for regeneration. Data were analyzed using the Biacore T200 Evaluation software (GE Healthcare Life Sciences).

Nuclear Magnetic Resonance (NMR) Measurement

For NMR measurements, recombinant mouse PrP 121–231 uniformly labeled with ^{15}N was prepared in 50 mM acetate-d_3 buffer (pH 4.8) containing 1 mM NaN_3 and 1 μM DSS dissolved in 99% H_2O/1% D_2O. NMR spectra were recorded at 25.0 °C on a Bruker Avance 600 spectrometer (Bruker BioSpin, Rheinstetten, Germany) at Gifu University. The spectrometer operated at a ^{1}H frequency of 600.13 MHz and a ^{15}N frequency of 60.81 MHz. A 5-mm ^{1}H inverse detection probe with triple-axis gradient coils was used for all measurements. ^{1}H-^{15}N HSQC spectra were acquired with 2048 complex points covering 9615 Hz for ^{1}H and 256 complex points covering 1521 Hz for ^{15}N. NMR data were processed using the TOPSPIN software package (Bruker BioSpin, Rheinstetten, Germany).

Docking Simulation

We performed docking simulation of Alp and Oxp with mouse PrP^{C} using AutoDock 4.2 [34]. The three-dimensional structure of PrP^{C} obtained from the Protein Data Bank (ID: 1AG2 [35]) was used as a receptor. The atomic structures of Alp and Oxp were downloaded from the PubChem website (https://pubchem.ncbi.nlm.nih.gov/) (CID-66368 for alprenolol and CID-71172 for oxprenolol), and the atomic structures of their enantiomers were also generated. A cubic space of 45 × 45 × 45 Å was used as a search region, covering the whole surface of PrP^{C}. In our docking simulation, 50 individual calculations were run with genetic algorithm (ga_run = 50), in each of which 10^{8} energy calculations were performed (ga_num_evals = 10^{8}). The lowest energy structure was selected as a potential binding structure with PrP^{C}.

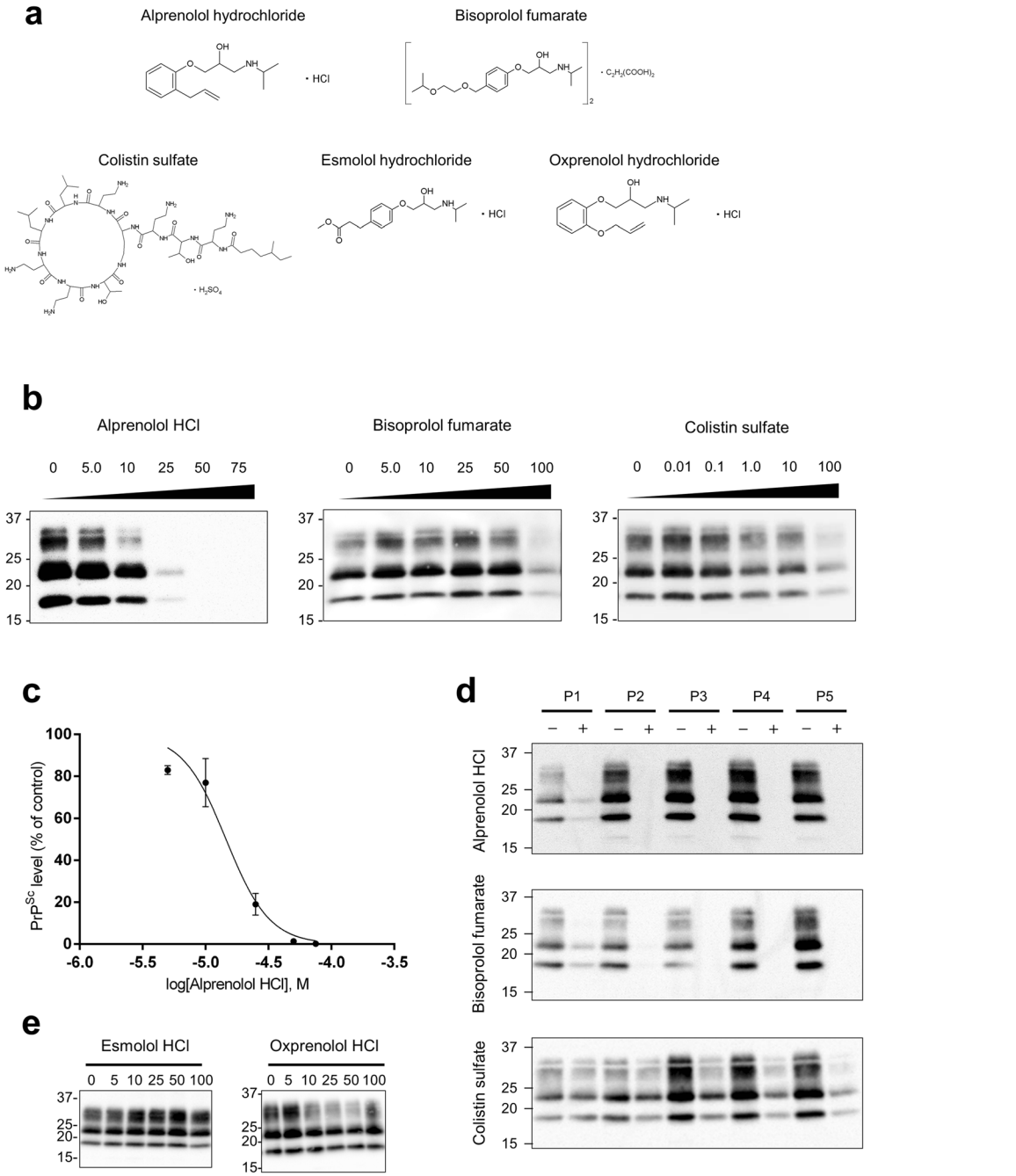

Fig. 1 Inhibitory effects of the candidate compounds on PrP^{Sc} accumulation in N2a-FK cells. **a** Structure of alprenolol hydrochloride, bisoprolol fumarate, colistin sulfate, esmolol hydrochloride and oxprenolol hydrochloride. **b** Inhibitory effects of alprenolol hydrochloride, bisoprolol fumarate, and colistin sulfate on PrP^{Sc} accumulation in N2a-FK cells. After the cells were incubated in medium mixed with each concentration of sample compound or water (negative control) for 48 h, the collected cell lysates were digested with proteinase K. Western blotting was then performed for quantification of the PrP^{Sc} level. **c** The intensity of each band was measured and expressed as a percentage of the negative control. Data are presented as the mean ± SD of three independent experiments. **d** Inhibitory effects of continued passage in the presence of alprenolol hydrochloride, bisoprolol fumarate, or colistin sulfate on PrP^{Sc} accumulation in N2a-FK cells. The cells were cultured in medium mixed with 50 μM of alprenolol hydrochloride, 100 μM of bisoprolol fumarate, or 100 μM of colistin sulfate, or original medium (negative control). The cells were passaged every 3 days and then the cell lysates were collected. After digestion with proteinase K, western blotting was performed to detect PrP^{Sc} accumulation. **e** PrP^{Sc} accumulation in N2a-FK cells after treatment with esmolol hydrochloride and oxprenolol hydrochloride. After the cells had been incubated in medium mixed with each concentration of sample compound or water (negative control) for 48 h, the collected cell lysates were digested with proteinase K. Western blotting was then performed for quantification of the PrP^{Sc} level

Statistical Analysis

One-way analysis of variance (ANOVA) followed by the Tukey–Kramer test was used for multiple comparisons. The log rank test was used to analyze the survival time of mice. All statistical analyses were performed using the Excel and GraphPad Prism software.

Results

Screening of the Drug by SPR Imaging

The 1200 FDA-approved drugs were screened to identify compounds with binding activity to human PrP^{C} using the Plexera PlexArray system. Recombinant human PrP 90–231 ($rHuPrP_{90–231}$) was applied to the library compounds immobilized on a sensor chip, and each affinity was measured. Thirty-one compounds showed dissociation constant (K_D) values of less than 1×10^{-6} M (Table 1), with dequalinium dichloride, alexidine dihydrochloride, and esmolol hydrochloride having the highest order K_D values (10^{-10}). Amphotericin B, which has been reported to inhibit PrP^{Sc} generation in scrapie-infected cultured cells and to prolong the course of the disease in animals [36, 37], was also shown to exhibit binding activity to PrP^{C}.

Anti-prion Effects of the Hit Compounds on Prion-Infected Cultured Cells

The inhibitory effects of the 31 hit compounds on prion-infected culture cells were examined using N2a58 cells persistently infected with Fukuoka-1 strain (Supplementary Fig. 1). The cells were incubated with each compound for 48 h at the indicated concentration, then the amount of PrP^{Sc} was quantified by western blotting after proteinase K digestion. We found that three compounds, alprenolol hydrochloride (Alp), bisoprolol fumarate (Bis), and colistin sulfate significantly reduced the level of PrP^{Sc} in the cultured cells (Fig. 1b). In addition, PrP^{Sc} completely disappeared after continued passage in the presence of Alp and Bis (Fig. 1d), both of which are β-adrenergic blockers used for the treatment of cardiovascular diseases. In particular, Alp exhibited strong anti-prion effects, with an IC_{50} value of 15 μM (Fig. 1c). Esmolol hydrochloride and oxprenolol hydrochloride (Oxp), that are also β-adrenergic blockers with similar structures to Bis and Alp respectively (Fig. 1a), did not exert anti-prion effects on the infected cells (Fig. 1e). The effect of colistin on prions was evident but weaker than that of Alp or Bis. The inhibitory effect of antimycin A, a mitochondrial inhibitor, could not be evaluated due to its potent cytotoxicity on prion-infected cultured cells.

Alprenolol Hydrochloride Reduces PrP^{Sc} in the Brains of Prion-Infected Mice

To evaluate the in vivo therapeutic effects of the identified anti-prion compound, animal experiments using prion-infected mice were performed. As Alp can penetrate the blood–brain barrier easier than Bis [38, 39], Alp was selected for the animal experiments. CD-1 mice intracerebrally infected with mouse-adapted human prion, Fukuoka-1, were orally administered drinking water containing Alp at 50 or 250 mg/L from the day after infection (half-life of Alp, ~2 h) [39]. At 115 days post infection (d.p.i.), some of the mice (control: $n = 3$; 250 mg/L: $n = 5$; 50 mg/L: $n = 3$) showing no symptoms of prion disease were euthanized to evaluate PrP^{Sc} accumulation and spongiform changes in the brain tissue. PrP^{Sc} levels in the mice treated with Alp were significantly lower than those of the control group (Fig. 2a). Immunohistochemistry showed reduced levels of PrP^{Sc} staining in brain sections from Alp-treated mice as compared with the control (Fig. 2b). There was a statistically significant decrease in the number of vacuoles in the cortex from the mice treated with 50 mg/L of Alp (Fig. 3a). Although there appears to be a dose-dependent decrease in the thalamus, the differences did not reach statistical significance. These results suggest that Alp has an inhibitory effect on PrP^{Sc} accumulation and spongiform changes in the mouse brain tissues at the middle stage of the disease (115 d.p.i), whereas the survival periods of the treated groups remained unchanged compared with the control (Fig. S2a, Table 2). In addition, similar levels of PrP^{Sc} accumulation and spongiform changes were observed in both groups at the terminal stage (Fig. S2b, c).

Conventional SPR and NMR Analysis Using Alprenolol Hydrochloride and Recombinant PrP

We investigated the binding kinetics of Alp and Bis to recombinant mouse PrP 23–231 ($rMoPrP_{23–231}$) by conventional SPR analysis using the Biacore T200 system (Fig. S3). In contrast to the previous screening by SPRi, the proteins were immobilized on a sensor chip as ligands and the compounds were injected into this system. The K_D value of the positive control, quinacrine, was 0.69 mM (Fig. S3b), whereas ampicillin, which is not known to have any anti-prion effects, had a low binding affinity to $rMoPrP_{23–231}$ (Fig. S3a). The K_D values of Alp and Bis could not be calculated due to their low binding ability (Fig. S3b). Analysis using $rHuPrP_{23–231}$ as the ligand also presented similar results (Fig. S4). In NMR analysis, there was no difference in the spectra of $rMoPrP_{121–231}$ with or without Alp, suggesting that the interaction between Alp and $rMoPrP_{121–231}$ was not detectable at pH 4.8 (Fig. S5).

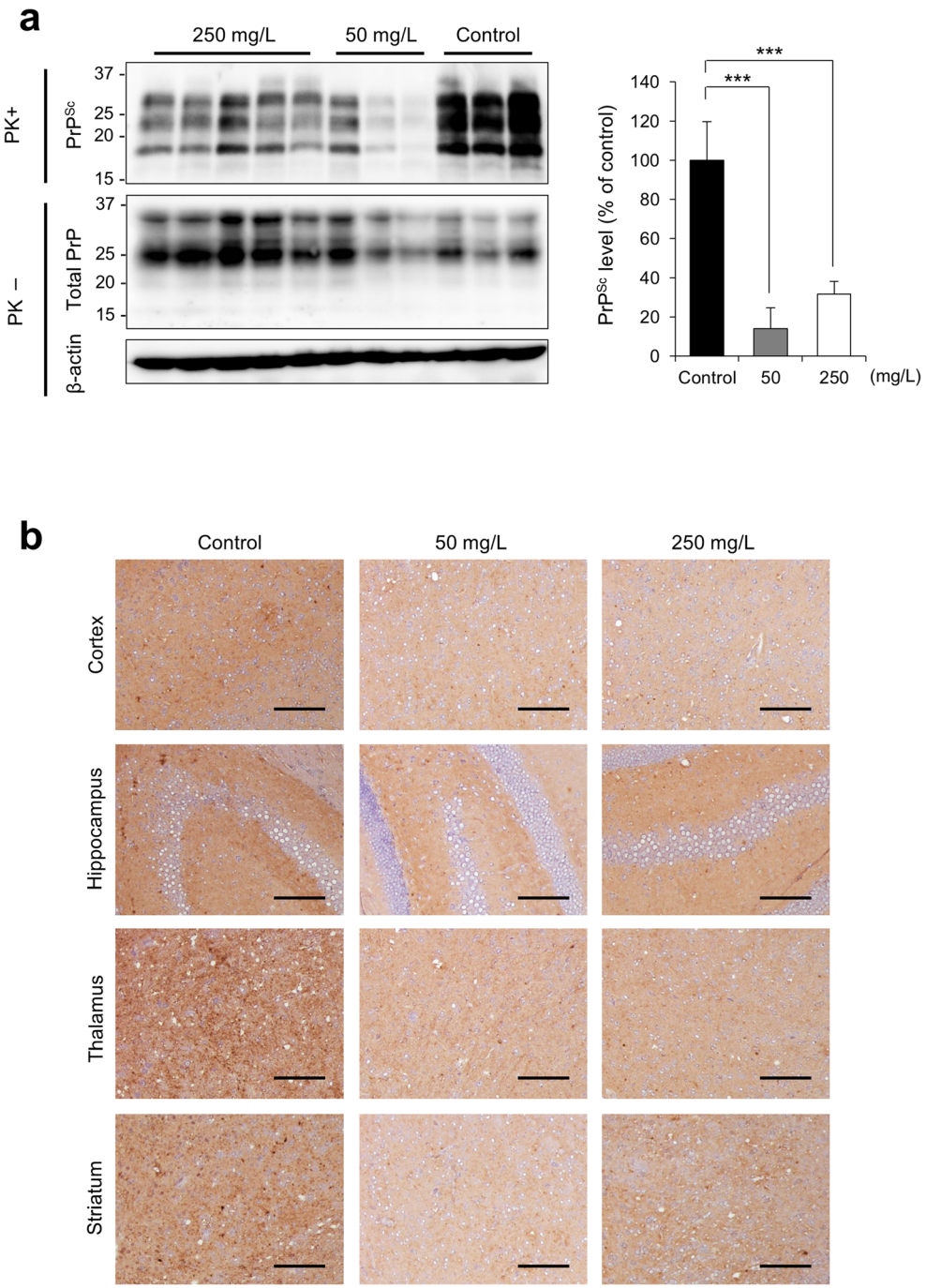

Fig. 2 Alprenolol hydrochloride reduces PrP^{Sc} accumulation in a mouse brain at 115 d.p.i. CD-1 mice were intracerebrally infected with strain Fukuoka-1. The following day, the mice were given drinking water containing alprenolol hydrochloride at 250 or 50 mg/L. Mice in the control group were given normal drinking water without the compound. At 115 d.p.i and the terminal stage, mice from each group were euthanized for brain homogenates and histopathological analysis (control: $n = 3$; 250 mg/L: $n = 5$; 50 mg/L: $n = 3$). **a** Western blotting of the brain homogenates at 115 d.p.i. was performed to quantify the PrP^{Sc} level. The intensity of each band was measured and expressed as a percentage of the control. The data are presented as the mean ± SD. Statistical analysis was determined using one-way ANOVA followed by the Tukey–Kramer test. ***$p < 0.001$ compared with the control. **b** Immunohistochemical staining of PrP^{Sc} of the brain slices at 115 d.p.i was performed. Scale bar, 100 μm

Docking Simulation of the Binding Structures of Alprenolol and PrP^{C}

To examine the binding structures of Alp with mouse PrP^{C}, we performed docking simulation using the software AutoDock 4.2 [34]. In Fig. 4, the binding structures obtained from the docking simulation are presented for Alp and Oxp and their enantiomers. The calculated binding positions were located around the helix-B for all of the molecules. This position was similar to the binding sites of other compounds that have previously been reported to have anti-prion activity [26, 28]. We noted that Alp (Fig. 4a) displays an additional interaction with a loop near helix-A, resulting in the formation of a bridging conformation. By contrast, Oxp, which had no anti-prion effect on the infected culture cells regardless of its structural similarities to Alp (Fig. 1a, e), did not show a clear interaction with regions other than helix-B. The calculated binding energies of Alp (− 5.68 and − 5.81 kcal/mol) were lower than those of Oxp (− 5.22 and − 4.83 kcal/mol) indicating the higher affinity of Alp.

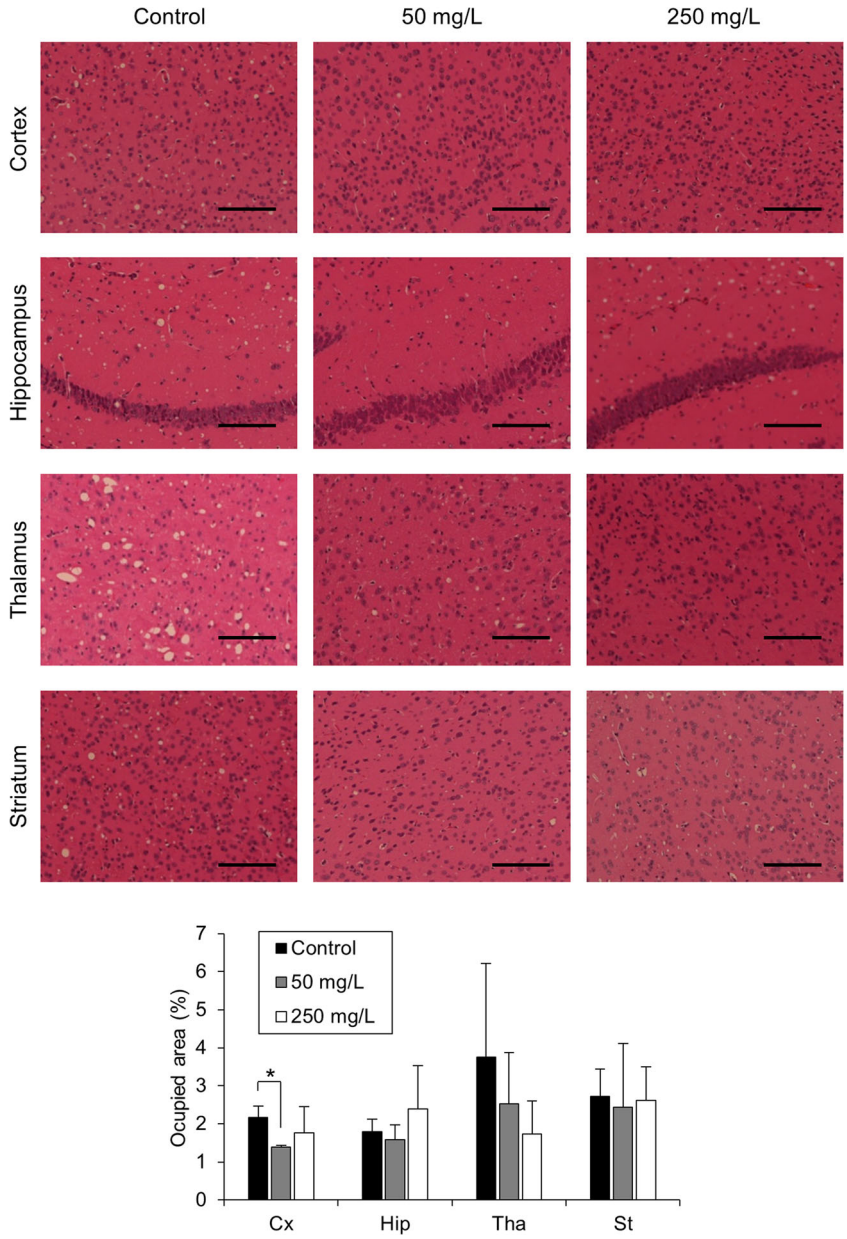

Fig. 3 Effects of alprenolol hydrochloride on the spongiform changes in mouse brains at 115 d.p.i. Hematoxylin and eosin staining of PrP^{Sc} in the brain sections at 115 d.p.i was performed. The areas occupied by vacuoles were quantified using the ImageJ software (cortex: Cx, hippocampus: Hip, thalamus: Tha, striatum: St). The data are presented as the mean ± SD. Statistical analysis was determined using one-way ANOVA followed by the Tukey–Kramer test. $*p < 0.05$ compared with the control. Scale bar, 100 μm

Discussion

In this study, we found that among the 31 compounds from the FDA-approved drug library showing binding activity in SPRi, three drugs, namely Alp, Bis, and colistin sulfate, exhibited anti-prion effects on prion-infected cultured cells. This type of drug repositioning approach can be promising because the safety and pharmacokinetics of existing drugs have already been fully determined. This approach avoids the risks of unknown adverse effects and saves considerable time and expense compared with de novo drug development [40]. Indeed, drug repositioning has been proposed for the development of drugs to treat prion diseases [22, 41].

In the first screening, we used the SPRi system to identify PrP-binding compounds from the drug library. Although Alp showed strong binding to $rHuPrP_{90–231}$ in this screening, much lower binding ability to both $rMoPrP_{23–231}$ and $rHuPrP_{23–231}$ was detected by conventional SPR analysis

Table 2 Survival periods of prion-infected mice administered with alprenolol hydrochloride

Mouse	Strain	Alprenolol HCl (mg/L)	Number	Mean ± SD (days)
CD-1	Fukuoka-1	0	7	168.4 ± 7.2
		250	9	164 ± 12.4
		50	10	162 ± 10.3

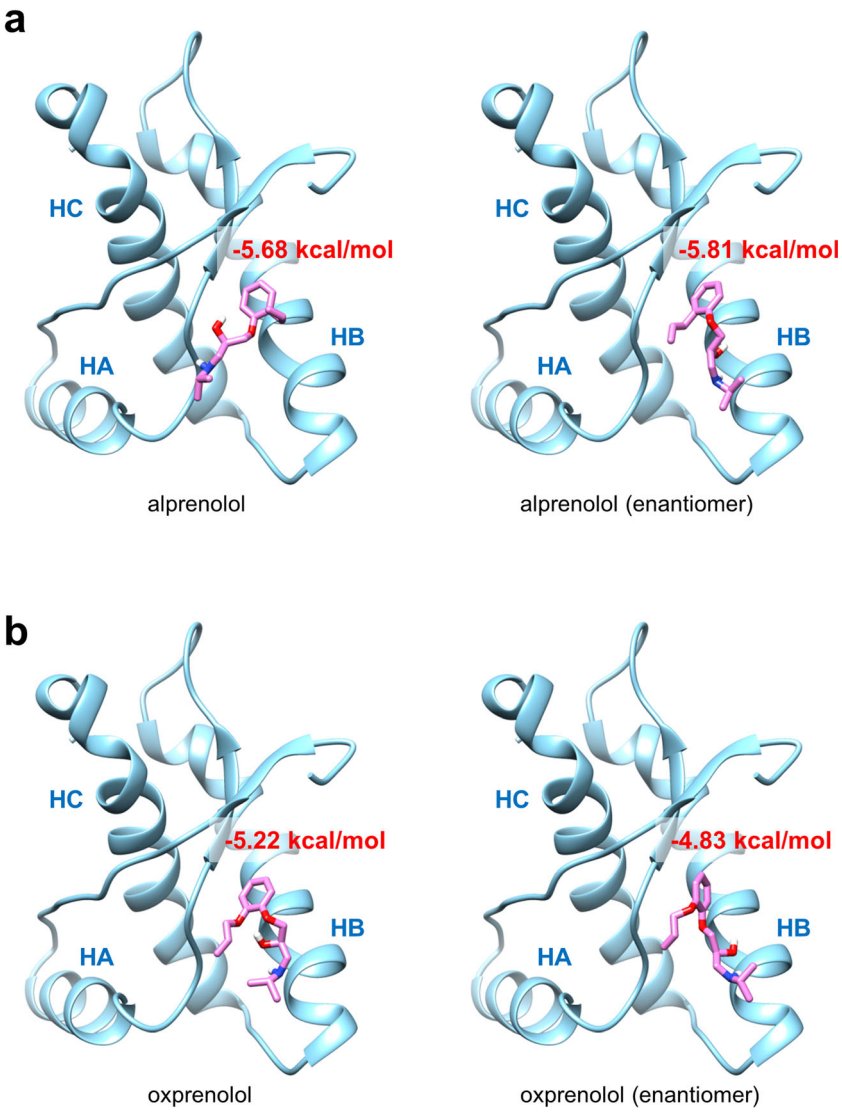

Fig. 4 Docking simulation of the interaction of alprenolol and oxprenolol with mouse PrP^C. Binding structures obtained by the docking simulation for alprenolol and its enantiomer (**a**) and oxprenolol and its enantiomers (**b**). PrP^C, including three helixes (HA, HB, and HC), is shown by a ribbon representation in light blue, and the compounds are shown by stick models. The calculated binding energies are also given

using the Biacore T200. As mentioned above, both of the SPR systems detected binding affinity between proteins and compounds based on reverse SPR mechanisms [30], which might explain the inconsistent results. The sensitivity of SPR was thought to depend on the mass of the analytes that bind to the ligands on the sensor chip. Higher molecular weight molecules induce larger reflection changes and are therefore more readily detected than small molecules. Since soluble proteins were used as analytes in SPRi, this assay might have relatively high sensitivity in the detection of molecular interactions compared with conventional SPR. However, both of the SPR technologies do not completely reproduce true physiological events in vivo because the proteins or compounds are chemically immobilized on a sensor chip in these systems. Moreover, little differences in the spectra of $rMoPrP_{121–231}$ with or without Alp were detectable by NMR analysis. It should be noted that NMR analysis was conducted only under acidic conditions (pH 4.8) due to the solubility of rMoPrP, making it difficult to determine the interaction between PrP and Alp under physiological pH conditions. Together, there is no clear evidence to prove that the anti-prion activity of Alp on infected cells and mice was attributed to its binding to PrP^C; however, the docking simulation suggests that Alp interacts with the hotspot of mouse PrP^C. This position is reported to be unstable and critical for pathogenic conversion of PrP [26, 42]. Notably, Oxp, which is similar in structure to Alp but has lower affinity, exhibited no inhibitory effects on PrP^{Sc} accumulation in prion-infected cells. The difference in structures between Alp and Oxp is only the integration of an oxygen into a side chain (Fig. 1a), suggesting that the structure of this side chain is important for the anti-prion effects of Alp. Alp formed a bridging conformation between helix-B and a loop near helix-A in the docking simulation. However, neither Oxp nor its enantiomer showed a clear interaction with regions other than helix-B. It has been reported that GN8 disrupts the salt bridge between Arg156 at the C-terminus of helix-A and

Glu196 in the loop between helix-B and helix-C and rearranges this interaction, leading to the conformational stability of PrP^C [42]. Our results suggest that the bridge structure formed by Alp might contribute to its anti-prion effects, similar to GN8. However, it is possible that Alp may have another target responsible for its anti-prion effects as well as PrP^C. Although esmolol hydrochloride and Oxp are also β-adrenergic blockers, neither presented clear inhibition of prion-infected cultured cells, indicating that β-adrenergic receptors are unlikely to be the targets of Alp. Further studies are required to reveal the underlying mechanisms of the anti-prion effects of Alp.

The reduction in PrP^{Sc} accumulation in the brains of Alp-treated mice at 115 d.p.i. was confirmed by western blotting and immunohistochemical staining. By contrast, Alp treatment did not prolong the survival periods. The inconsistencies in the data may be attributed in part to the remarkable reduction in water intake by the infected mice at the terminal stage. However, further studies are needed to assess the inhibitory effects of Alp on prion diseases under different experimental conditions such as other routes, doses, start points, and frequencies of Alp administration.

In conclusion, we identified PrP-binding compounds by SPRi screening. Among them, Alp showed anti-prion effects on prion-infected cultured cells and partially effects in mice. This SPRi approach is thought to be suitable for discovering effective drugs to treat neurodegenerative diseases caused by abnormal protein aggregation, such as prion diseases.

Acknowledgments We thank Atsuko Matsuo for the technical assistance. This work was supported by JSPS KAKENHI Grant Number JP15H04269 and a grant form Takeda Science Foundation.

We thank Kate Fox, DPhil, from Edanz Group (www.edanzediting.com/ac) for editing a draft of this manuscript.

Author Contributions Y.M., N.N., and R.A. designed the entire project. Y.M., T.I., Y.O.K, T.N., H.T., D.I., and K.K. performed the experiments and analyzed the data. N.N. and R.A. supervised and discussed the data. All authors reviewed the manuscript.

Compliance with Ethical Standards

All of these experiments were approved by the Committee on the Animal Care and Use Committees of Nagasaki University. The mice were cared for according to the Guidelines for Animal Experimentation of Nagasaki University

Conflict of Interest The authors declare that they have no conflicts of interest.

References

1. Prusiner SB (1982) Novel proteinaceous infectious particles cause scrapie. Science 216(4542):136–144
2. Prusiner SB (1998) Prions. Proc Natl Acad Sci U S A 95(23): 13363–13383
3. Rossi G, Salmona M, Forloni G, Bugiani O, Tagliavini F (2003) Therapeutic approaches to prion diseases. Clin Lab Med 23(1): 187–208
4. Weissmann C, Aguzzi A (2005) Approaches to therapy of prion diseases. Annu Rev Med 56:321–344. https://doi.org/10.1146/annurev.med.56.062404.172936
5. Aguzzi A, O'Connor T (2010) Protein aggregation diseases: pathogenicity and therapeutic perspectives. Nat Rev Drug Discov 9(3): 237–248. https://doi.org/10.1038/nrd3050
6. Vogtherr M, Grimme S, Elshorst B, Jacobs DM, Fiebig K, Griesinger C, Zahn R (2003) Antimalarial drug quinacrine binds to C-terminal helix of cellular prion protein. J Med Chem 46(17): 3563–3564. https://doi.org/10.1021/jm034093h
7. Doh-Ura K, Iwaki T, Caughey B (2000) Lysosomotropic agents and cysteine protease inhibitors inhibit scrapie-associated prion protein accumulation. J Virol 74(10):4894–4897
8. Haïk S, Brandel JP, Salomon D, Sazdovitch V, Delasnerie-Laupêtre N, Laplanche JL, Faucheux BA, Soubrié C et al (2004) Compassionate use of quinacrine in Creutzfeldt-Jakob disease fails to show significant effects. Neurology 63(12):2413–2415
9. Collinge J, Gorham M, Hudson F, Kennedy A, Keogh G, Pal S, Rossor M, Rudge P et al (2009) Safety and efficacy of quinacrine in human prion disease (PRION-1 study): a patient-preference trial. Lancet Neurol 8(4):334–344. https://doi.org/10.1016/S1474-4422(09)70049-3
10. Caughey B, Raymond GJ (1993) Sulfated polyanion inhibition of scrapie-associated PrP accumulation in cultured cells. J Virol 67(2): 643–650
11. Caughey B, Brown K, Raymond GJ, Katzenstein GE, Thresher W (1994) Binding of the protease-sensitive form of PrP (prion protein) to sulfated glycosaminoglycan and Congo red [corrected]. J Virol 68(4):2135–2141
12. Tsuboi Y, Doh-Ura K, Yamada T (2009) Continuous intraventricular infusion of pentosan polysulfate: clinical trial against prion diseases. Neuropathology 29(5):632–636. https://doi.org/10.1111/j.1440-1789.2009.01058.x
13. Doh-ura K, Ishikawa K, Murakami-Kubo I, Sasaki K, Mohri S, Race R, Iwaki T (2004) Treatment of transmissible spongiform encephalopathy by intraventricular drug infusion in animal models. J Virol 78(10):4999–5006
14. Bone I, Belton L, Walker AS, Darbyshire J (2008) Intraventricular pentosan polysulphate in human prion diseases: an observational study in the UK. Eur J Neurol 15(5):458–464. https://doi.org/10.1111/j.1468-1331.2008.02108.x
15. Haik S, Marcon G, Mallet A, Tettamanti M, Welaratne A, Giaccone G, Azimi S, Pietrini V et al (2014) Doxycycline in Creutzfeldt-Jakob disease: a phase 2, randomised, double-blind, placebo-controlled trial. Lancet Neurol 13(2):150–158. https://doi.org/10.1016/S1474-4422(13)70307-7
16. Tagliavini F, Forloni G, Colombo L, Rossi G, Girola L, Canciani B, Angeretti N, Giampaolo L et al (2000) Tetracycline affects abnormal properties of synthetic PrP peptides and PrP(Sc) in vitro. J Mol Biol 300(5):1309–1322. https://doi.org/10.1006/jmbi.2000.3840
17. Forloni G, Iussich S, Awan T, Colombo L, Angeretti N, Girola L, Bertani I, Poli G et al (2002) Tetracyclines affect prion infectivity. Proc Natl Acad Sci U S A 99(16):10849–10854. https://doi.org/10.1073/pnas.162195499
18. Peretz D, Williamson RA, Kaneko K, Vergara J, Leclerc E, Schmitt-Ulms G, Mehlhorn IR, Legname G et al (2001) Antibodies inhibit prion propagation and clear cell cultures of prion infectivity. Nature 412(6848):739–743. https://doi.org/10.1038/35089090
19. Heppner FL, Musahl C, Arrighi I, Klein MA, Rülicke T, Oesch B, Zinkernagel RM, Kalinke U et al (2001) Prevention of scrapie pathogenesis by transgenic expression of anti-prion protein antibodies.

Science 294(5540):178–182. https://doi.org/10.1126/science.1063093

20. White AR, Enever P, Tayebi M, Mushens R, Linehan J, Brandner S, Anstee D, Collinge J et al (2003) Monoclonal antibodies inhibit prion replication and delay the development of prion disease. Nature 422(6927):80–83. https://doi.org/10.1038/nature01457
21. Solforosi L, Criado JR, McGavern DB, Wirz S, Sánchez-Alavez M, Sugama S, DeGiorgio LA, Volpe BT et al (2004) Cross-linking cellular prion protein triggers neuronal apoptosis in vivo. Science 303(5663):1514–1516. https://doi.org/10.1126/science.1094273
22. Nakagaki T, Satoh K, Ishibashi D, Fuse T, Sano K, Kamatari YO, Kuwata K, Shigematsu K et al (2013) FK506 reduces abnormal prion protein through the activation of autolysosomal degradation and prolongs survival in prion-infected mice. Autophagy 9(9):1386–1394. https://doi.org/10.4161/auto.25381
23. Ishibashi D, Homma T, Nakagaki T, Fuse T, Sano K, Takatsuki H, Atarashi R, Nishida N (2015) Strain-dependent effect of macroautophagy on abnormally folded prion protein degradation in infected neuronal cells. PLoS One 10(9):e0137958. https://doi.org/10.1371/journal.pone.0137958
24. Moreno JA, Halliday M, Molloy C, Radford H, Verity N, Axten JM, Ortori CA, Willis AE et al (2013) Oral treatment targeting the unfolded protein response prevents neurodegeneration and clinical disease in prion-infected mice. Sci Transl Med 5(206):206ra138. https://doi.org/10.1126/scitranslmed.3006767
25. Halliday M, Radford H, Sekine Y, Moreno J, Verity N, le Quesne J, Ortori CA, Barrett DA et al (2015) Partial restoration of protein synthesis rates by the small molecule ISRIB prevents neurodegeneration without pancreatic toxicity. Cell Death Dis 6:e1672. https://doi.org/10.1038/cddis.2015.49
26. Kuwata K, Nishida N, Matsumoto T, Kamatari YO, Hosokawa-Muto J, Kodama K, Nakamura HK, Kimura K et al (2007) Hot spots in prion protein for pathogenic conversion. Proc Natl Acad Sci U S A 104(29):11921–11926. https://doi.org/10.1073/pnas.0702671104
27. Hyeon JW, Choi J, Kim SY, Govindaraj RG, Jam Hwang K, Lee YS, An SS, Lee MK et al (2015) Discovery of novel anti-prion compounds using in silico and in vitro approaches. Sci Rep 5:14944. https://doi.org/10.1038/srep14944
28. Ishibashi D, Nakagaki T, Ishikawa T, Atarashi R, Watanabe K, Cruz FA, Hamada T, Nishida N (2016) Structure-based drug discovery for prion disease using a novel binding simulation. EBioMedicine 9:238–249. https://doi.org/10.1016/j.ebiom.2016.06.010
29. Neumann T, Junker HD, Schmidt K, Sekul R (2007) SPR-based fragment screening: advantages and applications. Curr Top Med Chem 7(16):1630–1642
30. Nguyen HH, Park J, Kang S, Kim M (2015) Surface plasmon resonance: a versatile technique for biosensor applications. Sensors (Basel) 15(5):10481–10510. https://doi.org/10.3390/s150510481
31. Pickhardt M, Neumann T, Schwizer D, Callaway K, Vendruscolo M, Schenk D, St George-Hyslop P, Mandelkow EM et al (2015) Identification of small molecule inhibitors of tau aggregation by targeting monomeric tau as a potential therapeutic approach for tauopathies. Curr Alzheimer Res 12(9):814–828
32. Ishibashi D, Atarashi R, Fuse T, Nakagaki T, Yamaguchi N, Satoh K, Honda K, Nishida N (2012) Protective role of interferon regulatory factor 3-mediated signaling against prion infection. J Virol 86(9):4947–4955. https://doi.org/10.1128/JVI.06326-11
33. Atarashi R, Moore RA, Sim VL, Hughson AG, Dorward DW, Onwubiko HA, Priola SA, Caughey B (2007) Ultrasensitive detection of scrapie prion protein using seeded conversion of recombinant prion protein. Nat Methods 4(8):645–650. https://doi.org/10.1038/nmeth1066
34. Morris GM, Huey R, Lindstrom W, Sanner MF, Belew RK, Goodsell DS, Olson AJ (2009) AutoDock4 and AutoDockTools4: automated docking with selective receptor flexibility. J Comput Chem 30(16):2785–2791. https://doi.org/10.1002/jcc.21256
35. Riek R, Hornemann S, Wider G, Billeter M, Glockshuber R, Wüthrich K (1996) NMR structure of the mouse prion protein domain PrP(121-231). Nature 382(6587):180–182. https://doi.org/10.1038/382180a0
36. Pocchiari M, Schmittinger S, Masullo C (1987) Amphotericin B delays the incubation period of scrapie in intracerebrally inoculated hamsters. J Gen Virol 68(Pt 1):219–223. https://doi.org/10.1099/0022-1317-68-1-219
37. Mangé A, Nishida N, Milhavet O, McMahon HE, Casanova D, Lehmann S (2000) Amphotericin B inhibits the generation of the scrapie isoform of the prion protein in infected cultures. J Virol 74(7):3135–3140
38. Bühring KU, Sailer H, Faro HP, Leopold G, Pabst J, Garbe A (1986) Pharmacokinetics and metabolism of bisoprolol-14C in three animal species and in humans. J Cardiovasc Pharmacol 8(Suppl 11):S21–S28
39. Hakkarainen JJ, Jalkanen AJ, Kääriäinen TM, Keski-Rahkonen P, Venäläinen T, Hokkanen J, Mönkkönen J, Suhonen M et al (2010) Comparison of in vitro cell models in predicting in vivo brain entry of drugs. Int J Pharm 402(1–2):27–36. https://doi.org/10.1016/j.ijpharm.2010.09.016
40. Ashburn TT, Thor KB (2004) Drug repositioning: identifying and developing new uses for existing drugs. Nat Rev Drug Discov 3(8):673–683. https://doi.org/10.1038/nrd1468
41. Halliday M, Radford H, Zents KAM, Molloy C, Moreno JA, Verity NC, Smith E, Ortori CA et al (2017) Repurposed drugs targeting eIF2α-P-mediated translational repression prevent neurodegeneration in mice. Brain 140:1768–1783. https://doi.org/10.1093/brain/awx074
42. Yamamoto N, Kuwata K (2009) Regulating the conformation of prion protein through ligand binding. J Phys Chem B 113(39):12853–12856. https://doi.org/10.1021/jp905572w